TRAJECTORY JITTER AND SINGLE BUNCH BEAM BREAK UP INSTABILITY

P. Craievich, S. Di Mitri#, Sincrotrone Trieste, Trieste, Italy
M. Borland, Argonne National Laboratory, Argonne, IL 60439, U. S. A.
A. A. Zholents, Lawrence Berkeley National Laboratory, Berkley, CA, 94720, U.S.A.

Abstract

This paper addresses stability issues related to control of the single bunch beam break up (SBBU) instability in the FERMI@Elettra linac using local trajectory bumps [1]. Analytical study and simulations using the code **elegant** are presented. Three different parameters have been used to characterize the SBBU, i.e. the projected emittance, the bunch head-to-tail deviation, and the Courant-Snyder amplitude for the slice centroid. It is shown that shot-to-shot trajectory jitter in the injector affects the efficiency of the control of the BBU.

MACHINE LATTICE AND JITTER BUDGET

Figure 1 shows the FERMI@elettra beam delivery system in its standard layout that includes two magnetic chicanes called BC1 and BC2 interleaved by 14 accelerating sections in the main linac (injector excluded). The motion in the high energy transfer line is not considered in this paper.

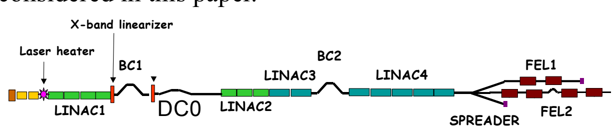

Figure 1: FERMI@elettra layout.

Main parameters of the Medium Length Bunch produced by the double compression scheme (MLB 2BC) are listed in Table 1.

Table 1: MLB 2BC main parameters used for simulations presented in this paper

Total charge	0.8	nC
Initial length, FW	9	ps
Final length, FW	1.4	ps
Initial peak current	80	A
Final peak current	800	A
Final energy	1.14	GeV

A perturbed machine lattice has been generated with static transverse misalignments (150 µm rms for magnets and 300 µm rms for linac structures), magnet rolls (0.5 mrad rms), and magnet field errors (0.01% rms). The trajectory distortion in Linac3 and Linac4 induces the SBBU due to the high impedance of the sections. For this reason, trajectory bumps have been applied to reduce the bunch head-tail deviation at the linac end below 1 rms beam size to achieve a projected normalised emittance of 1.5 µm.

Starting from this reference scenario, **elegant** [2] has been used to simulate shot-to-shot trajectory jitter. The launching error jitter, which may be generated by the jitter of the photo-cathode laser pointing stability, is not expected to exceed 10% of the beam size if the machine is properly tuned. Therefore, the rms launching position variation is 38 µm and the divergence variation is 2 µrad.

Other contributions to the trajectory jitter are quadrupole vibrations, short-term magnetic field variation, and shot-to-shot variation of the parasitic dispersion. For the quadrupole vibrations, an rmsamplitude of 0.44 µm [3], integrated over the frequency range 1 – 100 Hz (FERMI will nominally operate at 50 Hz) leads to an rms variation of the induced angular kick per quadrupole of 0.18 µrad (for a typical integrated strength kl=0.4 m^{-1}). The relative short term (<100 Hz) stability of the quadrupole gradient is 10^{-4} that induces an angular kick of 40 nrad for a relative beam offset of 1 mm inside the magnet. The variation of the parasitic dispersion induced by the quadrupole gradient variation is even smaller, $\Delta D \cong l \cdot \Delta\theta/2 \cong 4$ nm; even in case of 1% energy spread, the dispersive trajectory variation is in the sub-nm level. The last two terms are therefore negligible.

PROJECTED EMITTANCE

The geometric transverse wake field in the accelerating sections is taken as uniform over the whole transverse beam size, that is, we use a simple dipole wake. Hence, the slice emittance is preserved, while the projected emittance is not because the wake field drives a bunch tail oscillation relative to the bunch head; in this way, a correlation is established between the longitudinal slice position and its lateral displacement (banana shape). Let us assume a full width beam size of 4σ. The SBBU instability is considered suppressed if the head-tail deviation is smaller than 1σ that is their ratio is R≤1. This case is equivalent to an increase of the beam size by 25%, that is, a projected emittance growth of 50%, since $\varepsilon \sim \sigma^2$.

Figure 2 shows the normalised emittance when the launching coordinates of the bunch centroid move along an ellipse of semi-axes u = 76 µm and u' = 4 µrad in the (u, u') phase space with u=x,y. The phase advance in this space is defined by $u = A\cos\Delta\phi$. The maximum

#simone.dimitri@elettra.trieste.it

emittance growth is 44% in the horizontal plane and 64% in the vertical plane. (The lack of periodicity in the data results from the static errors in our initial configuration.)

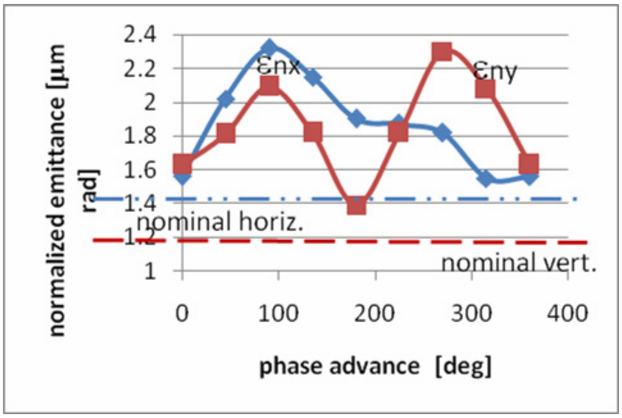

Figure 2: Normalized emittance growth at the linac end due to launching error jitter. The abscissa is the phase advance Δϕ in the transverse phase space. Dynamics in the *x* and *y* plane has been studied separately (geometric coupling has been neglected).

BANANA SHAPE

Figure 3 shows the banana shape jitter generated by the trajectory jitter defined in the first Section of this paper.

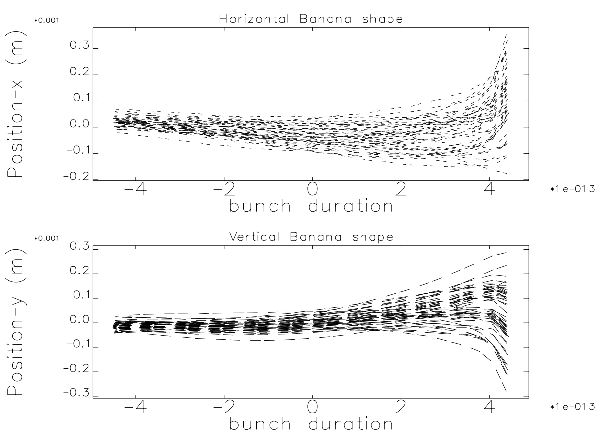

Figure 3: Banana shape (slice centroid lateral deviation vs. arrival time in 100 fs unit) at the linac end affected by trajectory jitter. The bunch head is on the left. The maximum head-tail deviation is 180 µm in the horizontal plane and 240 µm in the vertical plane.

Table 2: Statistic of the banana shape calculated over 50 jittered runs (see, Figure 3). R=(head-tail deviation)/(rms beam size). The rms beam sizes in the unperturbed case are: σ_x=140µm and σ_y =100µm

	R_x	R_y
AVE	0.9	1.1
RMS	0.4	0.8

Table 2 summarizes the statistics of the head-tail excursion over the 50 jittered runs shown in Figure 3 in terms of the ratio R. As already stated, the instability is considered suppressed if $\tilde{R} = \left|\langle R\rangle\right| + \sqrt{\langle R^2\rangle} \le 1$. Thus, according to Table 2 the instability jitter in the horizontal plane is close to the threshold, while the vertical plane is above it. This result is consistent with the evaluation of the projected emittance shown in the previous Section.

SLICE CENTROID AMPLITUDE

If the instability is suppressed at the linac end, that is the slice centroid transverse offset and divergence are small, then the bunch maintains its shape in the (t,x) and (t,y) plane at any point of the line downstream. On the contrary, if the banana shape is pronounced the slice optics in the bunch tail is mismatched to the magnetic lattice. Then, the bunch tail starts additional betatron oscillations around the head axis and the banana shape at any point downstream will depend on the Twiss parameters at the point of observation. So, the Courant-Snyder amplitude of the slice centroid may be introduced as a parameter to characterize the instability:

$$\varepsilon_{SC,u} = \gamma_u u_{cm}^2 + 2\alpha_u u_{cm} u'_{cm} + \beta_u u'^2_{cm} \qquad (1)$$

Let us focus on the horizontal plane, $u=x$. Same considerations apply to the vertical. This quantity provides a measure of the amplitude of motion that is independent of betatron phase. Its square root is proportional to the amplitudes of the slice centroid betatron motion x_{SC}, which represents the banana shape in Figure 3. In general x_{SC} is the linear superposition of three main contributions (see, Figure 4): i) the betatron motion, $x_{S\beta}$, generated by focusing; ii) the trajectory distortion, x_{ST}; iii) the transverse wake field effect, x_{SW}. Regarding the BBU instability, only the motion relative to the bunch head is of interest; thus, we define a new slice centroid invariant relative to the bunch head motion in eq.(2):

$$\varepsilon_{SW,x} = \gamma_x\left(x_{SC}-x_{offset}\right)^2 + 2\alpha_x\left(x_{SC}-x_{offset}\right)\left(x'_{SC}-x'_{offset}\right) + \beta_x\left(x'_{SC}-x'_{offset}\right)^2$$

where $x_{offset}= x_{S\beta}+ x_{ST}$ is considered to be constant along the bunch.

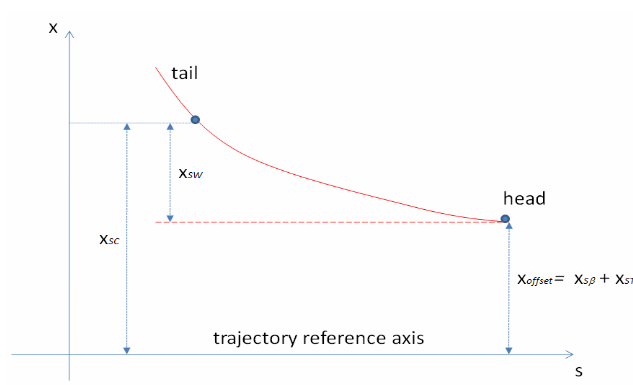

Figure 4: Contributions to the transverse motion of the slice centroid in presence of SBBU instability. x_{SW} is the slice centroid displacement relative to the bunch head.

The effect of the trajectory jitter on the scheme of SBBU suppression can be evaluated by looking at the shot-to-shot variation of the centroid amplitude ε_{SW} over the bunch duration. In fact, we require that the rms (over all jittered runs) slice lateral deviation be less than the rms (over all particles) beam size σ_x:

$$\frac{\sqrt{< x_{SW}^2 >}}{\sigma_x} \leq 1 \qquad (3)$$

Notice that $\sqrt{< x_{SW}^2 >} \sim \sqrt{< \varepsilon_{SW,x} >}\sqrt{\beta_x}\cos\varphi_x$. Then, eq.(3) is made more stringent by:

$$\sqrt{\frac{< \varepsilon_{SW,x} >}{\varepsilon_x}} \leq 1 \qquad (4)$$

where ε_x is the beam projected emittance.

The ratio defined by eq. (4) is plotted in Figure 5 for both the transverse planes. These results are consistent with those shown previously. Moreover, they offer a deeper and more complete understanding of the behaviour of the SBBU instability in presence of trajectory jitter. First, the projected emittance analysis does not contain the information on the slice particle distribution. In this case, a large emittance can be due to a small portion of the bunch tail that is not interested by the FEL process. Second, the parameter R defined above works with the projection of the banana shape onto the plane of interest and the jitter of the slice centroid position and divergence is treated separately. Eq.(4), instead, contains all the information of the slice phase space jitter at once.

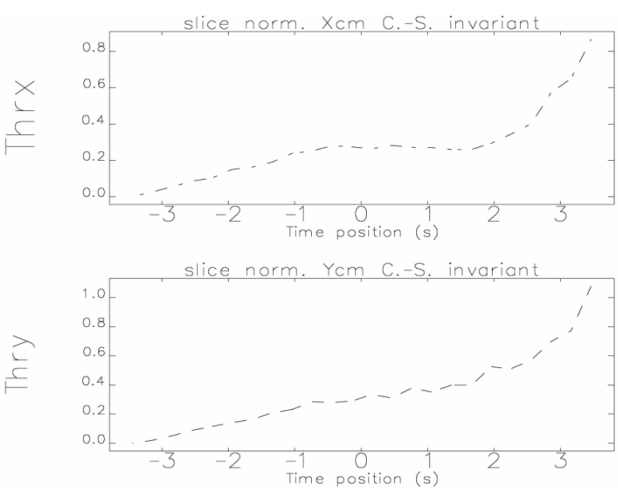

Figure 5: Ratio defined by eq.(4) vs. arrival time (in 100 fs unit) at the linac end affected by trajectory jitter. The ratio is below the unit threshold in the horizontal plane and slightly above in the vertical plane.

As expected from theory [4], the nonlinear behavior of the wake potential makes the banana shape more pronounced in a restricted region of the bunch length, far from the head. Figure 5 shows that, according to the long term error budget and to the short-to-shot jitter assumed in this paper, the instability is really critical only for a portion of the bunch length smaller than 10%.

CONCLUSIONS

The effect of the trajectory jitter, generated by the launching error jitter and by the quadrupole vibrations, on the SBBU instability has been studied in the FERMI linac. As a first step, the projected emittance growth at the linac end has been calculated as function of the launching error. Then, the jitter of the banana shape has been simulated and the deviation of the bunch head-tail lateral deviation has been evaluated. Finally, the jitter of the slice centroid Courant-Snyder amplitude along the bunch has been studied. A new parameter has been introduced which defines the amount of jitter of each slice transverse phase space in presence of SBBU instability.

The three methods, the projected emittance, the head-tail deviation and the slice centroid Courant-Snyder invariant give consistent results and, in the given order, they provide more and more information on the coupled transverse/longitudinal dynamics of the electron bunch.

Simulations predict that the SBBU instability is dominated by the jitter of the launching error. For a given machine error budget and jitter budget, the SBBU instability remains suppressed in the horizontal plane and for at least 90% of the bunch length in the vertical plane.

REFERENCES

[1] S. Di Mitri, A. Zholents, Trajectory correction in the Fermi@elettra linac, this conference.

[2] M. Borland, APS LS-287 (2000).

[3] S. Di Mitri, FPRD n.1 (June 2007).

[4] P. Craievich and S. Di Mitri, Proc. of EPAC 2006, Edinburgh, Scotland, UK (2006).

ACKNOWLEDGEMENT

The authors thank M. Cornacchia for very useful discussions and suggestions during the drafting of this work.

This work was supported in part by the Italian Ministry of University and Research under grants FIRB-RBAP045JF2 and FIRB-RBAP06AWK3.